Electronic Supplementary Information

Synthesis, structure and ROP capability of a tetra(amidine)bis(zirconium) calix[8]arene complex

William Clegg,[a] Mark R. J. Elsegood,[b] and Carl Redshaw[c]*

[a] *Chemistry, School of Natural & Environmental Sciences, Newcastle University, Newcastle upon Tyne NE1 7RU, U.K.*

[b] *Chemistry Department, Loughborough University, Loughborough, Leicestershire, LE11 3TU, U.K.*

[c] *Department of Chemistry, Graduate School of Science, Tokyo Metropolitan University, 1-1 Minami Osawa, Hachioji, Tokyo, 192-0397, Japan*

Contents

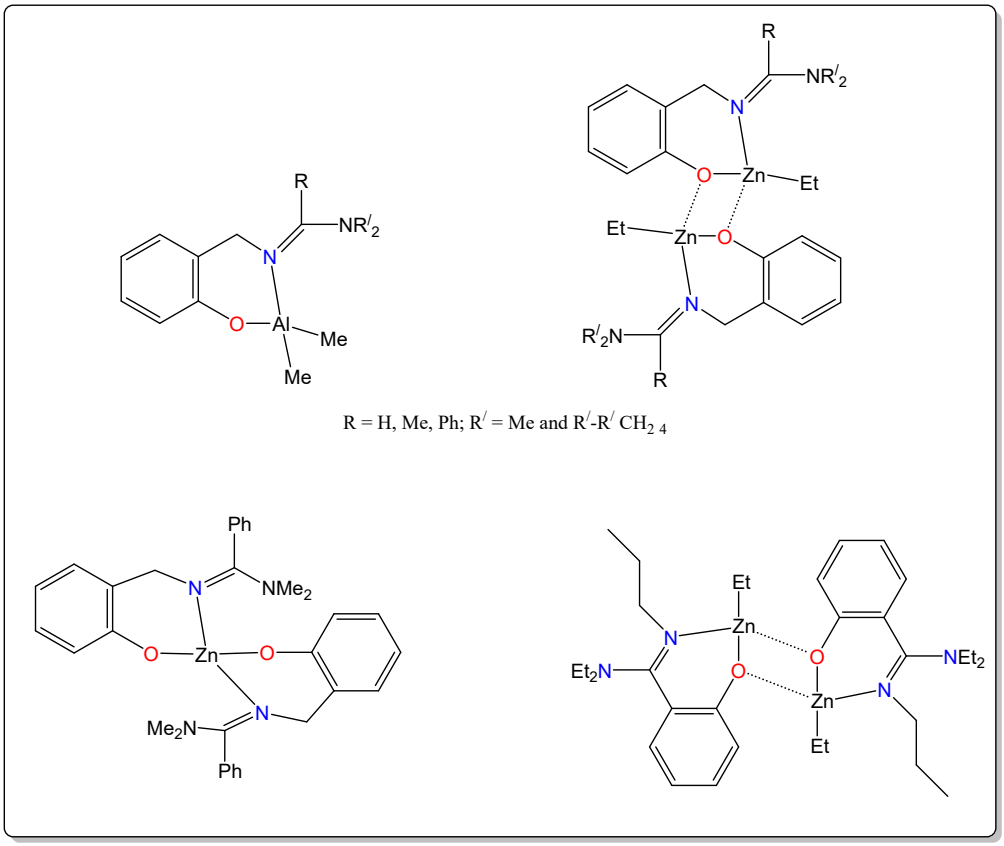

Figure S1. Aluminium and zinc amidates **I** to **IV**.[S1-S4]

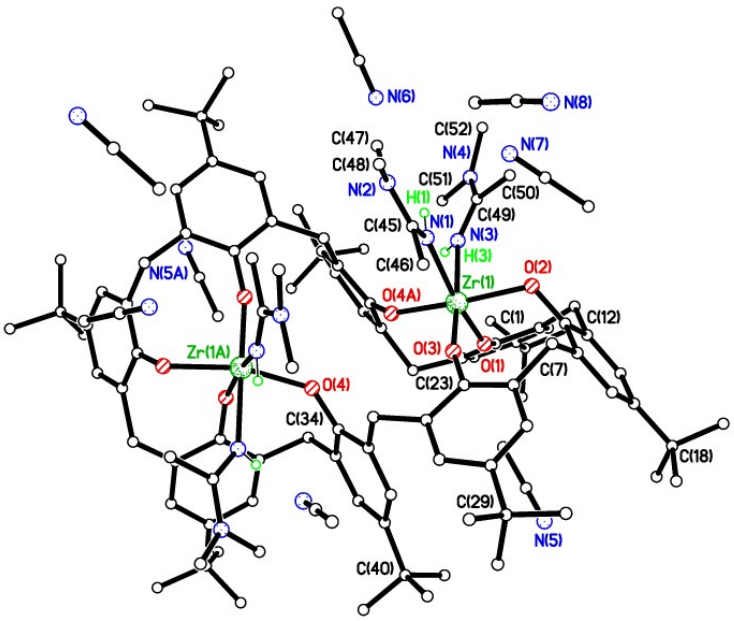

Figure S2. The molecular structure of $\{Zr[NHC(Me)NMe_2]_2\}_2L \cdot 7.25MeCN$ including solvent of crystallisation.

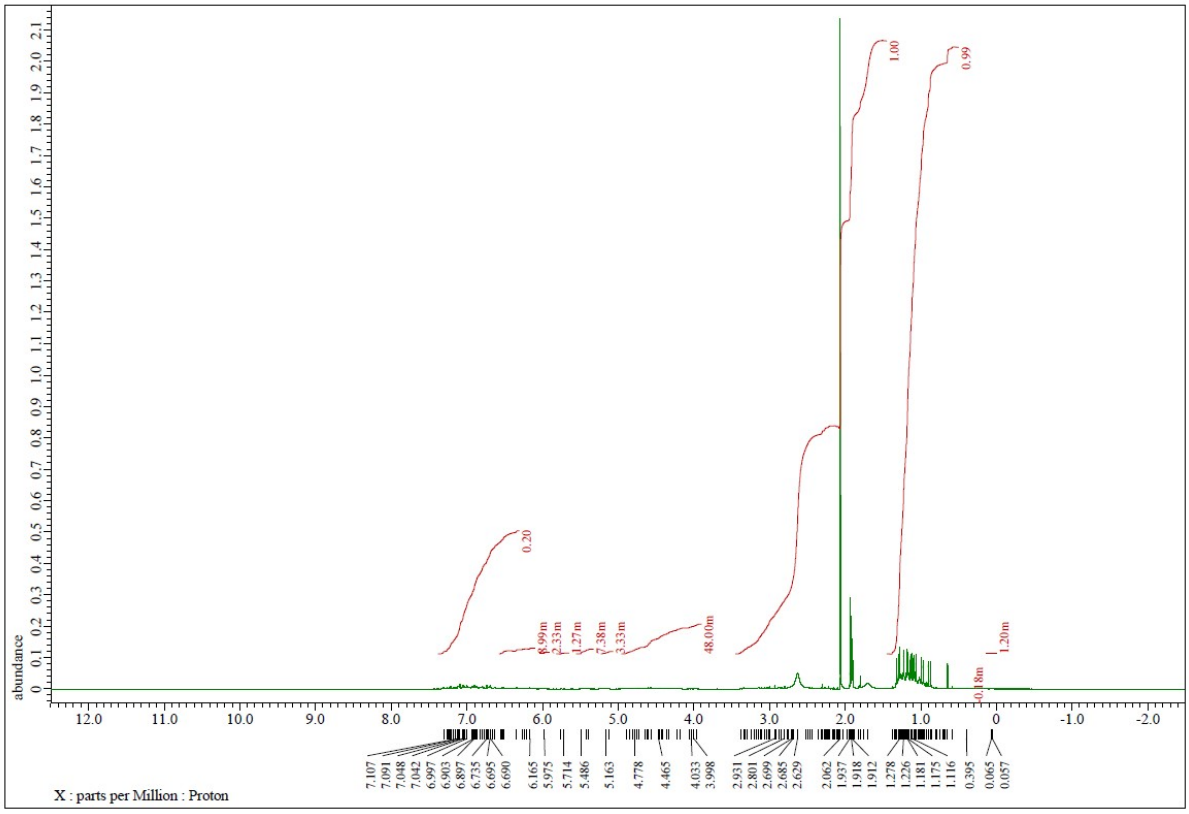

Figure S3. ^{1}H NMR spectrum (400 MHz, 298 K) of **1**·7.25MeCN in CD_3CN. Assignments include overlapping multiplets between 7.45 – 5.90 ppm (aryl*H*, 16H, See Fig. S4), 5.78 – 3.00 (*endo* and *exo*-CH_2, 16H, see Fig. S4 and S5), 2.63 (bs, 24H, *Me*$_2$N), 2.06 (s, 21.75H, *Me*CN), 1.71 (bs, 12H, *Me*N), 1.28 – 0.64 (multiple* s, 72H, *Me*$_3$C). * The number of singlets indicates conformational flexibity in solution.

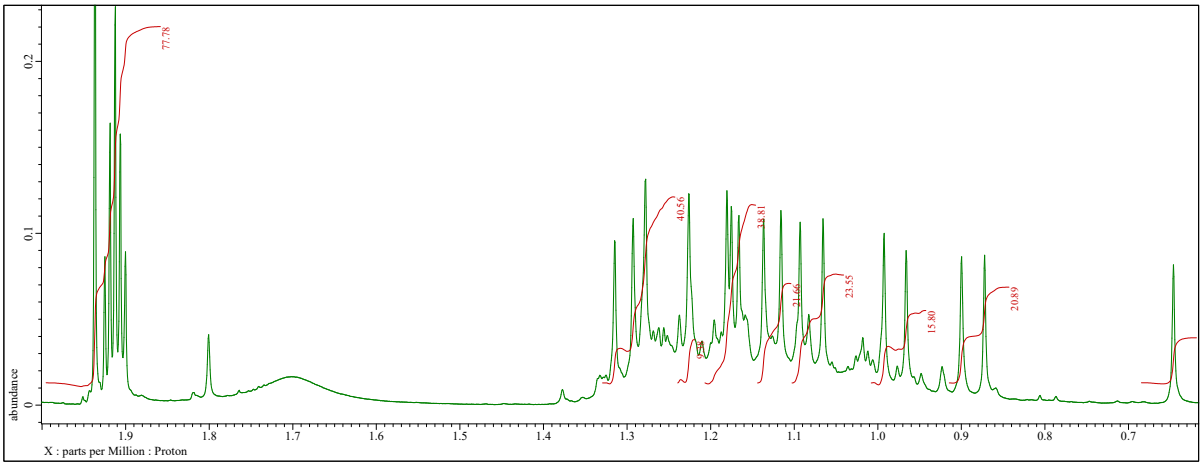

Figure S4. Expanded region 1.95 to 0.60 ppm of the ^{1}H NMR spectrum of **1**·7.25MeCN.

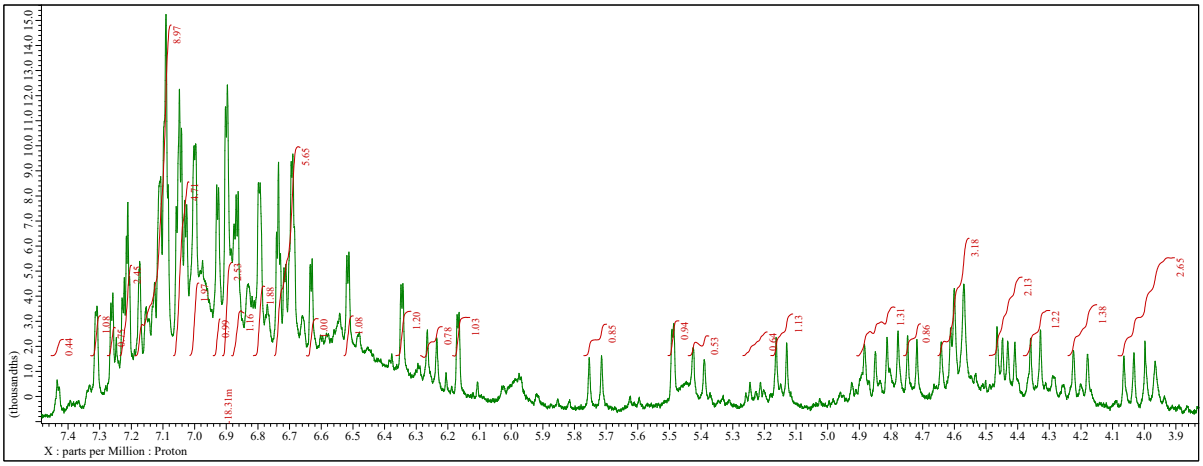

Figure S5. Expanded region 7.45 to 3.85 ppm of the ^{1}H NMR spectrum of **1**·7.25MeCN.

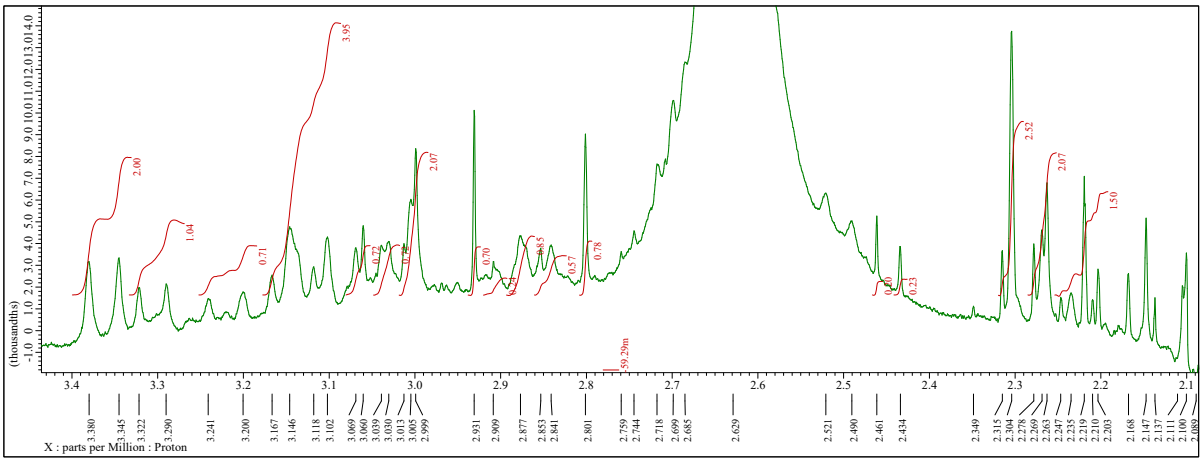

Figure S6. Expanded region 3.40 to 2.10 ppm of the ^{1}H NMR spectrum of **1**·7.25MeCN.

^{1}H NMR spectra and kinetics for the ε-CL runs using **1**:

Table S1: Conversion data for PCL using **1**:

Time (min)	Conversion (%)	ln[CL]0/[CL]t
15	0.76	0.007629027
30	4.51	0.046148656
45	10.58	0.111825815
60	20.7	0.231932057
75	32.05	0.386398045
90	43.1	0.563874845
105	53.76	0.771324962
120	62.5	0.980829253
135	67.11	1.112001526

Figure S7. PCL kinetics using **1** at t = 15 mins:

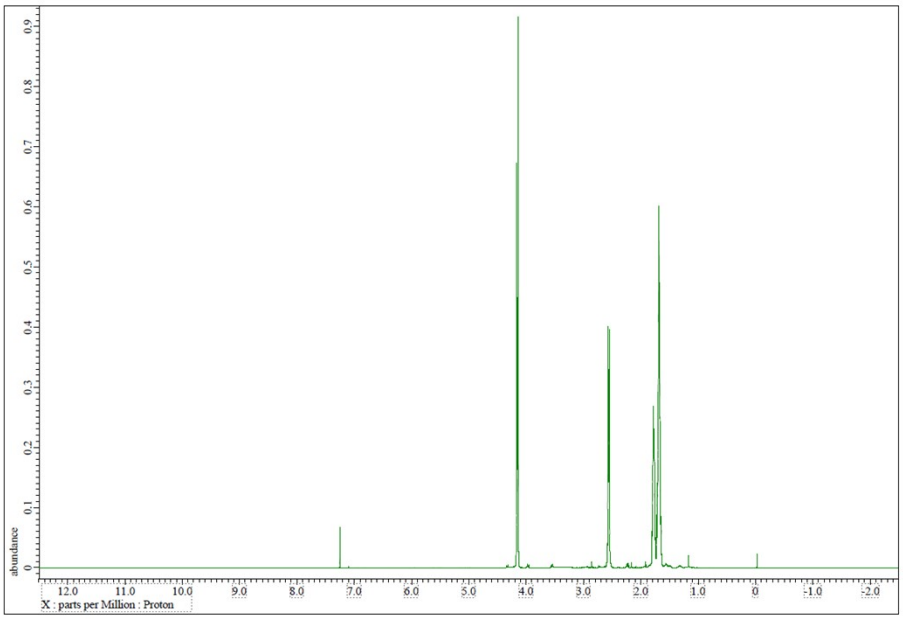

Figure S8. PCL kinetics using **1** at t = 30 mins:

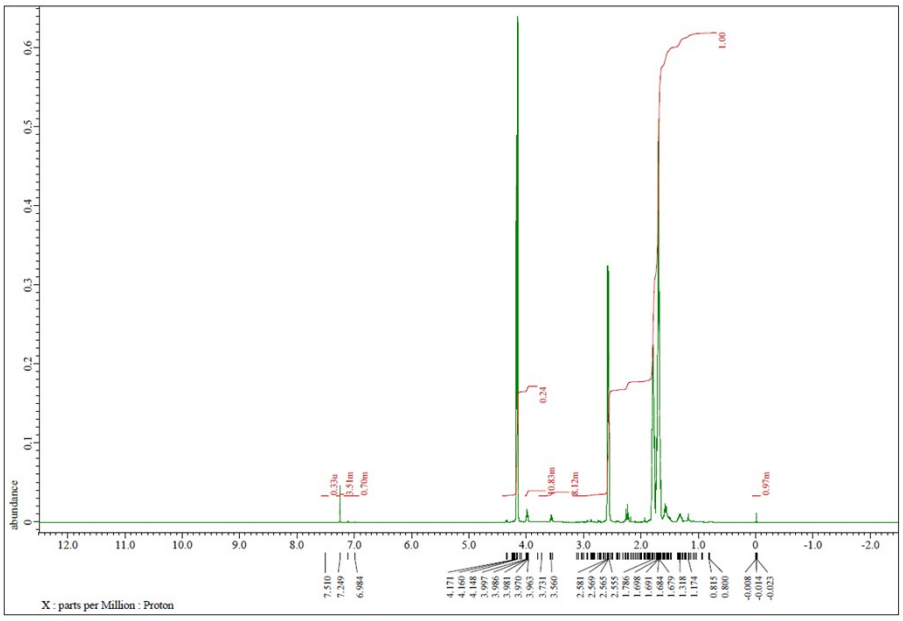

Figure S9. PCL kinetics using **1** at t = 45 mins:

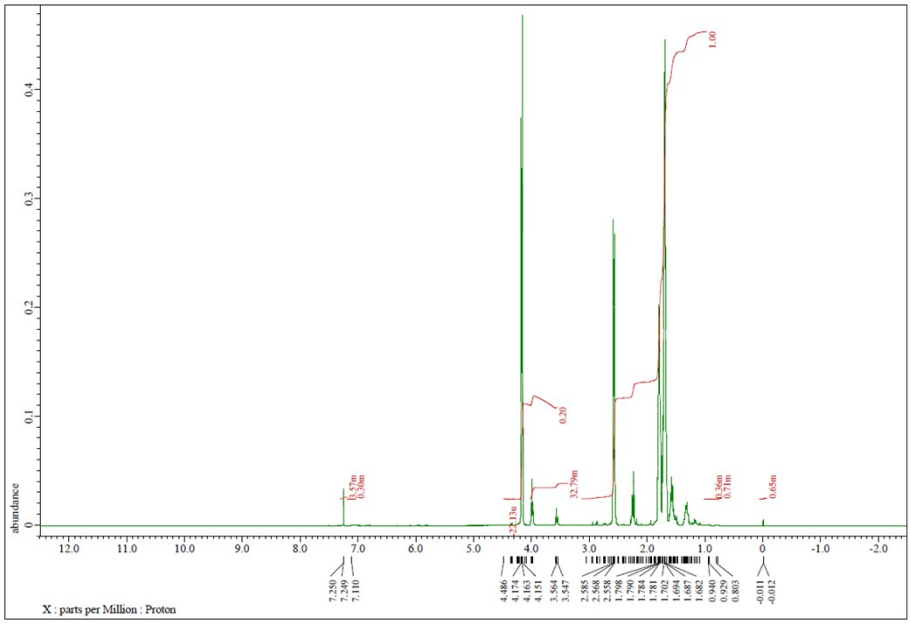

Figure S10. PCL kinetics using **1** at t = 60 mins:

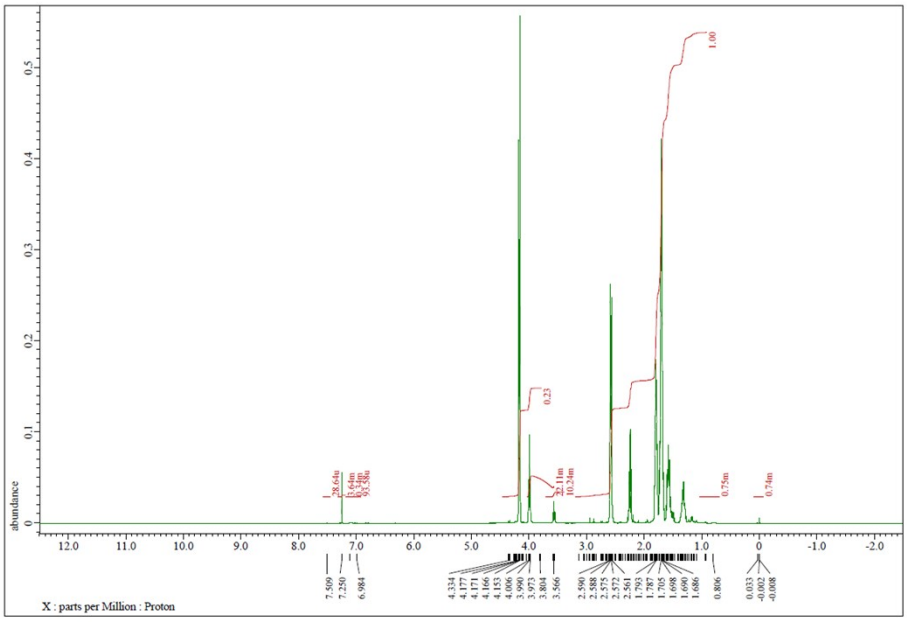

Figure S11. PCL kinetics using **1** at t = 75 mins:

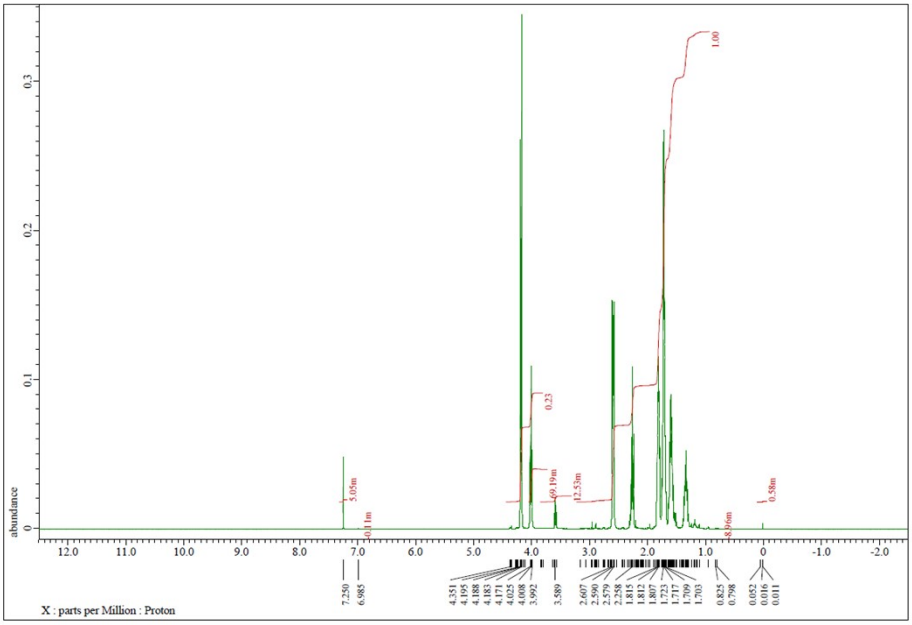

Figure S12. PCL kinetics using **1** at t = 90 mins:

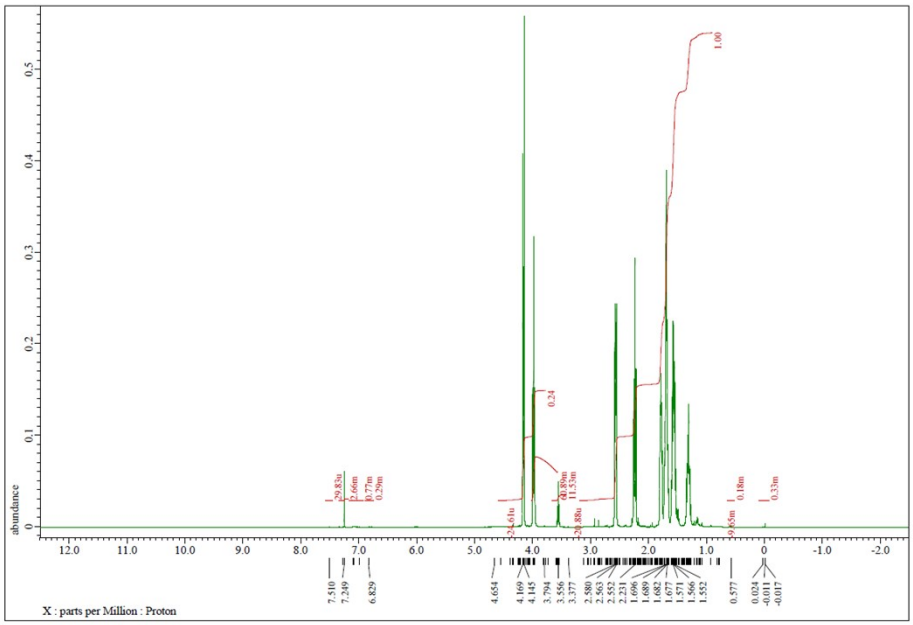

Figure S13. PCL kinetics using **1** at t = 105 mins:

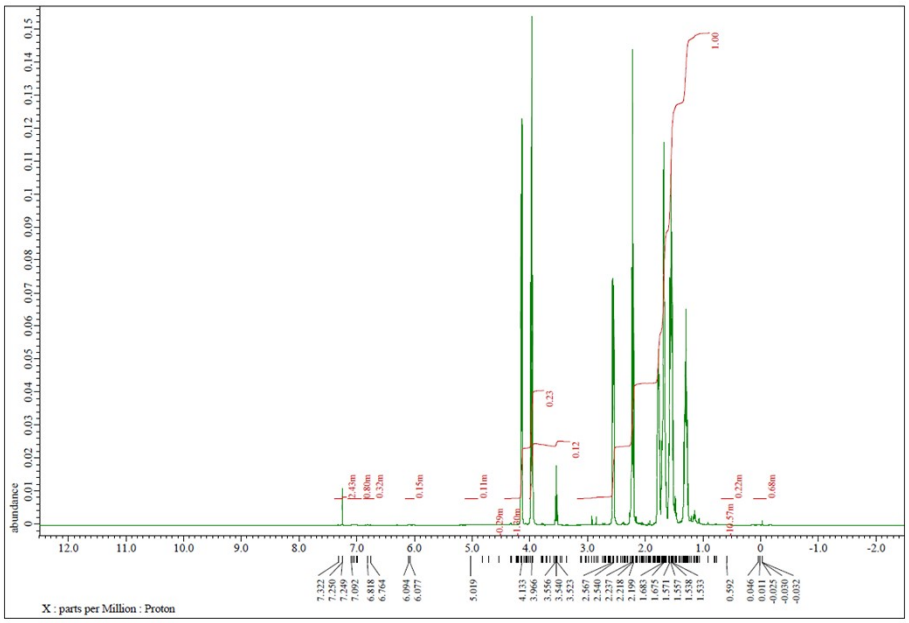

Figure S14. PCL kinetics using **1** at t = 120 mins:

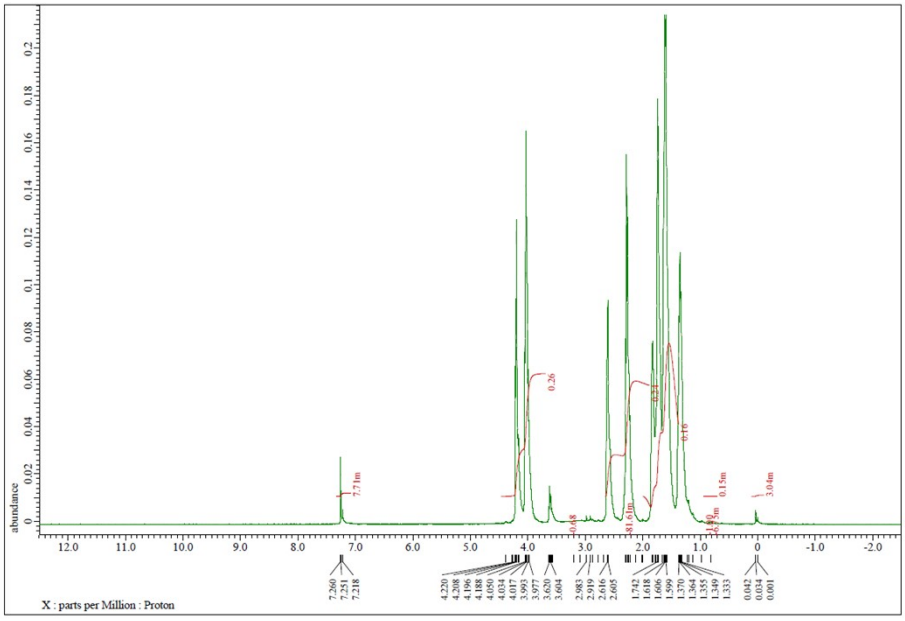

Figure S15. PCL kinetics using **1** at t = 135 mins:

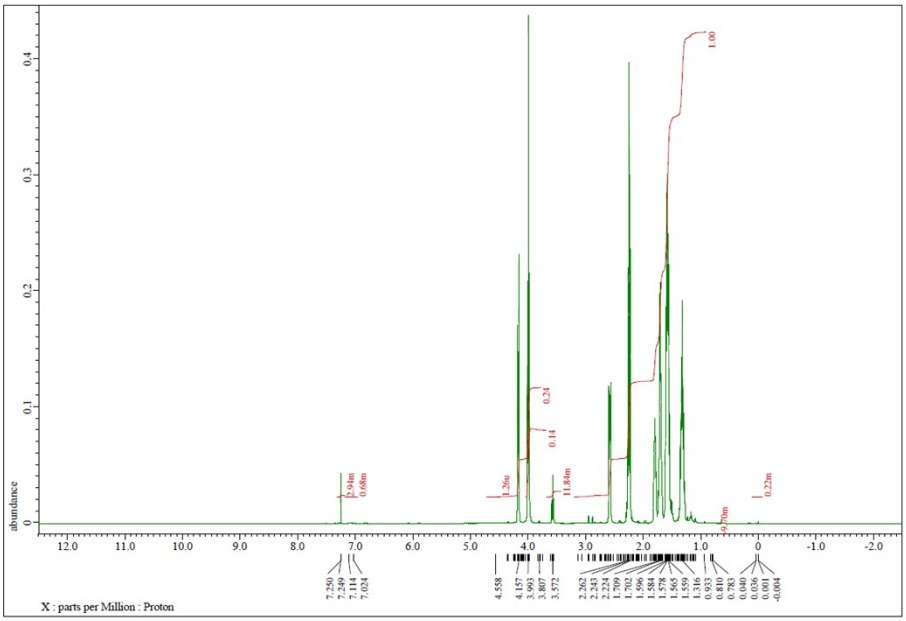

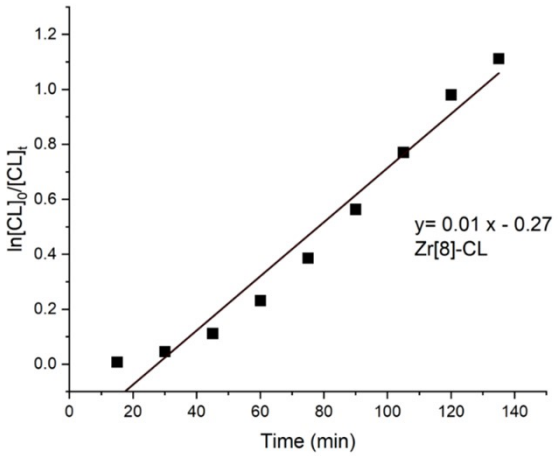

Figure S16. Kinetics graph for PCL using **1**.

For $[Zr(NMe_2)_4]$

Table S2. Conversion data for PCL using $[Zr(NMe_2)_4]$:

Time (min)	Conversion (%)	ln[CL]0/[CL]t
20	0.6	0.006018072
30	0.64	0.006420568
45	0.91	0.009141658
60	1.12	0.011263192
75	1.35	0.013591954
90	1.6	0.016129382
105	1.94	0.01959065
120	2.29	0.023166278
135	2.6	0.026343975
150	2.9	0.029428811

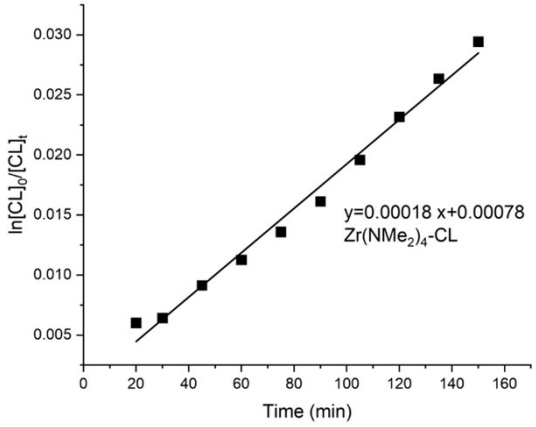

Figure S17. Kinetics graph for PCL using [$Zr(NMe_2)_4$].

For LH_8:

Table S3. Conversion data for PCL using LH_8:

Time (h)	Conversion (%)	ln[CL]0/[CL]t
1	0.7	0.007024615
2	0.71	0.007125325
3	0.72	0.007226045
4	0.74	0.007427516
5	0.76	0.007629027
6	0.78	0.007830579
7	0.8	0.008032172
8	0.82	0.008233805
9	0.84	0.008435479
10	0.86	0.008637193

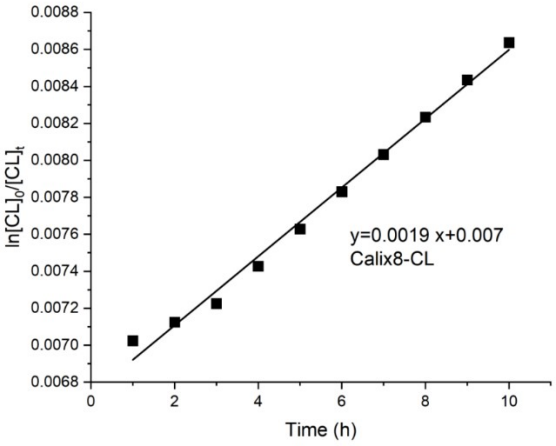

Figure S18. Kinetics graph for PCL using LH_8.

Individual ^1H NMR spectra and kinetics for the δ-VL runs

For **1**:

Table S4. Conversion data for PVL using **1**.

Time (h)	Conversion (%)	ln[VL]0/[VL]t
1	6.73	0.069671673
2	14.16	0.152685088
3	19.96	0.222643676
4	26.81	0.312111386
5	37.73	0.473690417
6	41.84	0.541972353

Figure S19. PVL kinetics using **1** at t = 1h:

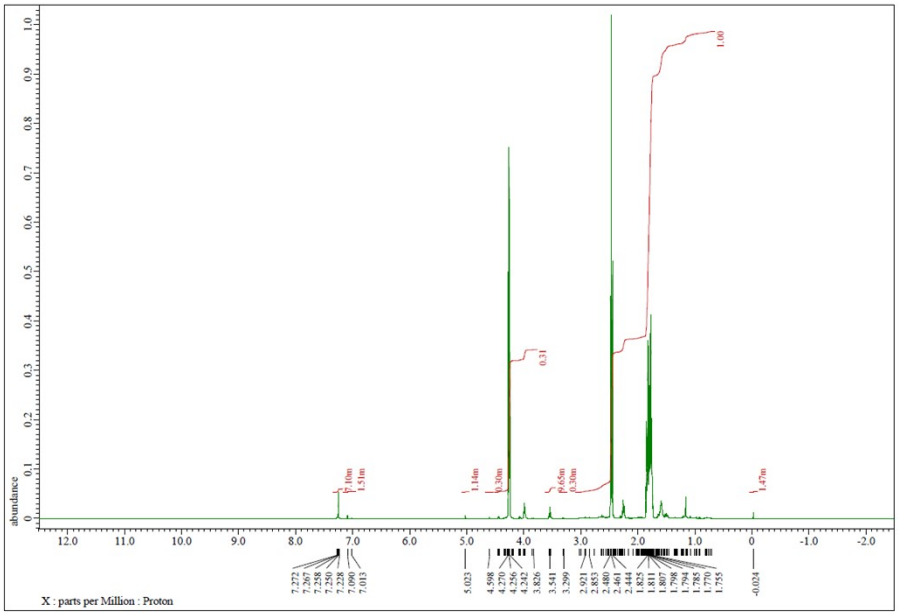

Figure S20. PVL kinetics using **1** at t = 2h:

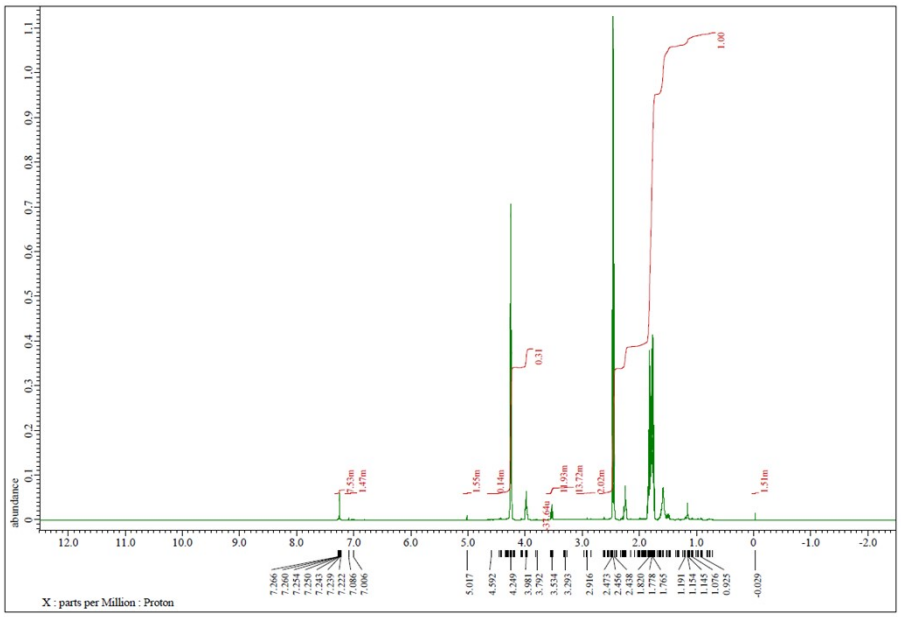

Figure S21. PVL kinetics using **1** at t = 3h:

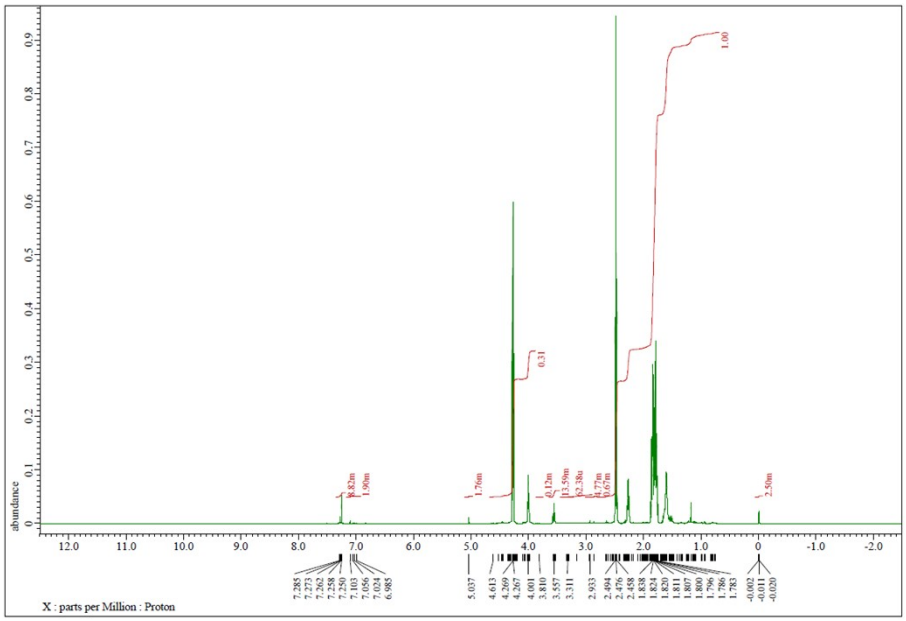

Figure S22. PVL kinetics using **1** at t = 4h:

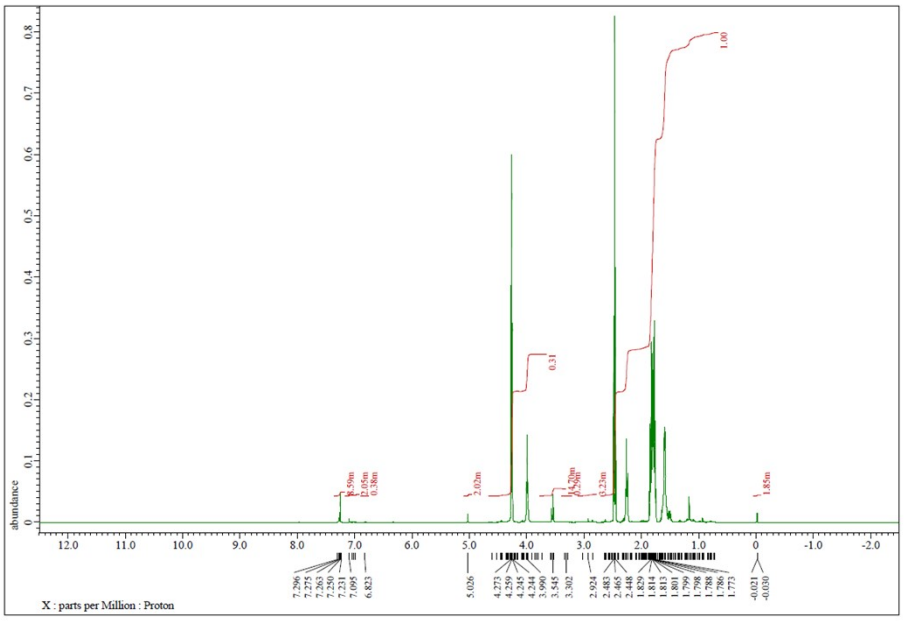

Figure S23. PVL kinetics using **1** at t = 5h:

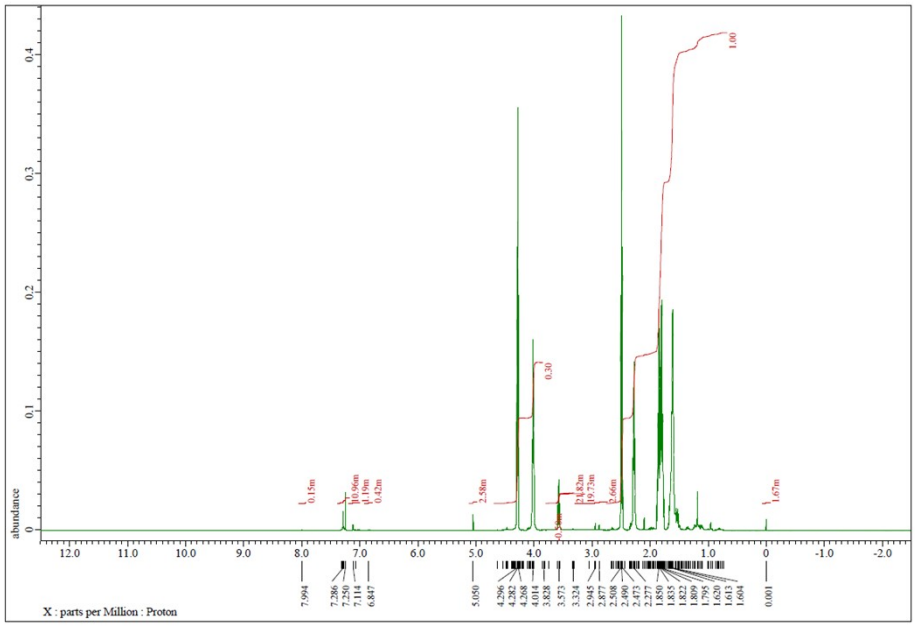

Figure S24. PVL kinetics using **1** at t = 6h:

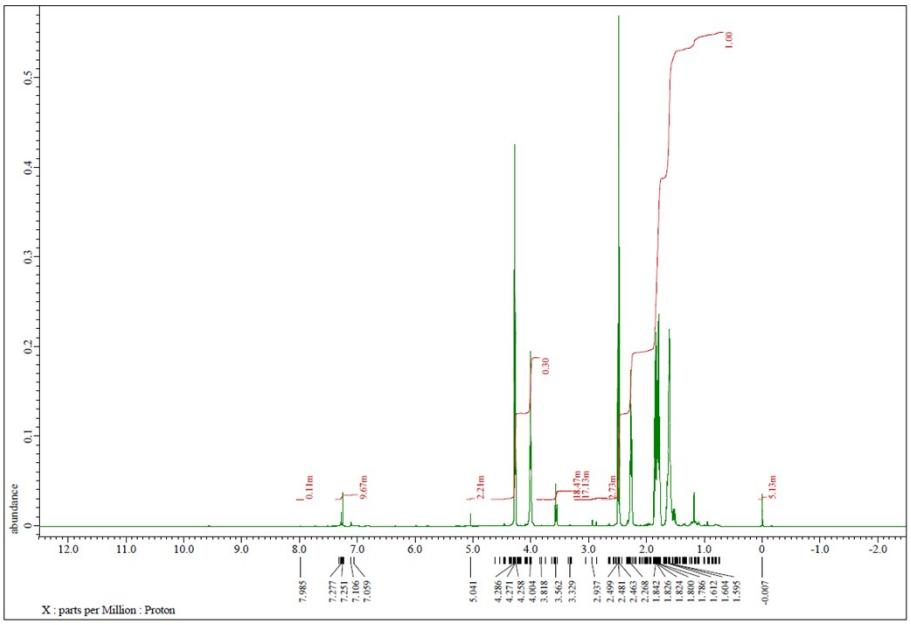

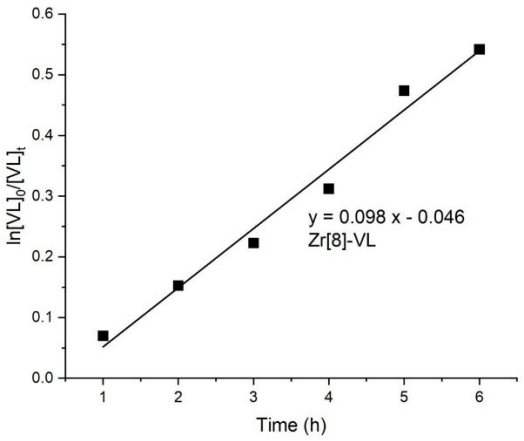

Figure S25. PVL kinetics graph using **1**.

For [$Zr(NMe_2)_4$}:

Table S5. Conversion data for PVL using [$Zr(NMe_2)_4$].

Time (h)	Conversion (%)	ln[VL]0/[VL]t
1	0.58	0.005816885
2	0.61	0.006118681
3	0.65	0.006521217
4	0.69	0.006923915
5	0.75	0.007528266

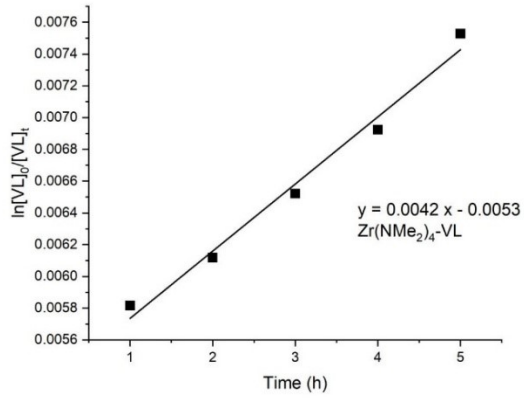

Figure S26. PVL kinetics graph using [$Zr(NMe_2)]_4$.

For LH_8:

Table 6. Conversion data for PVL using LH_8.

Time (h)	Conversion (%)	ln[VL]0/[VL]t
1	0.52	0.005213567
2	0.55	0.005515181
3	0.6	0.006018072
4	0.64	0.006420568
5	0.69	0.006923915
6	0.74	0.007427516
7	0.8	0.008032172

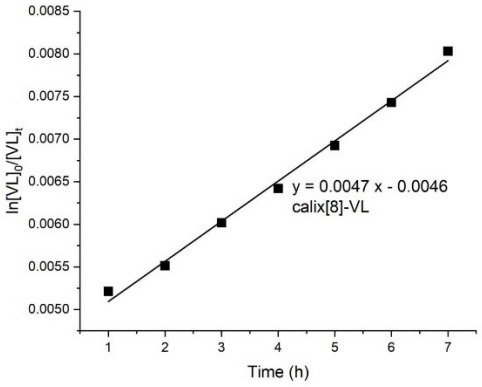

Figure S27. Kinetics graph for PVL using LH_8.

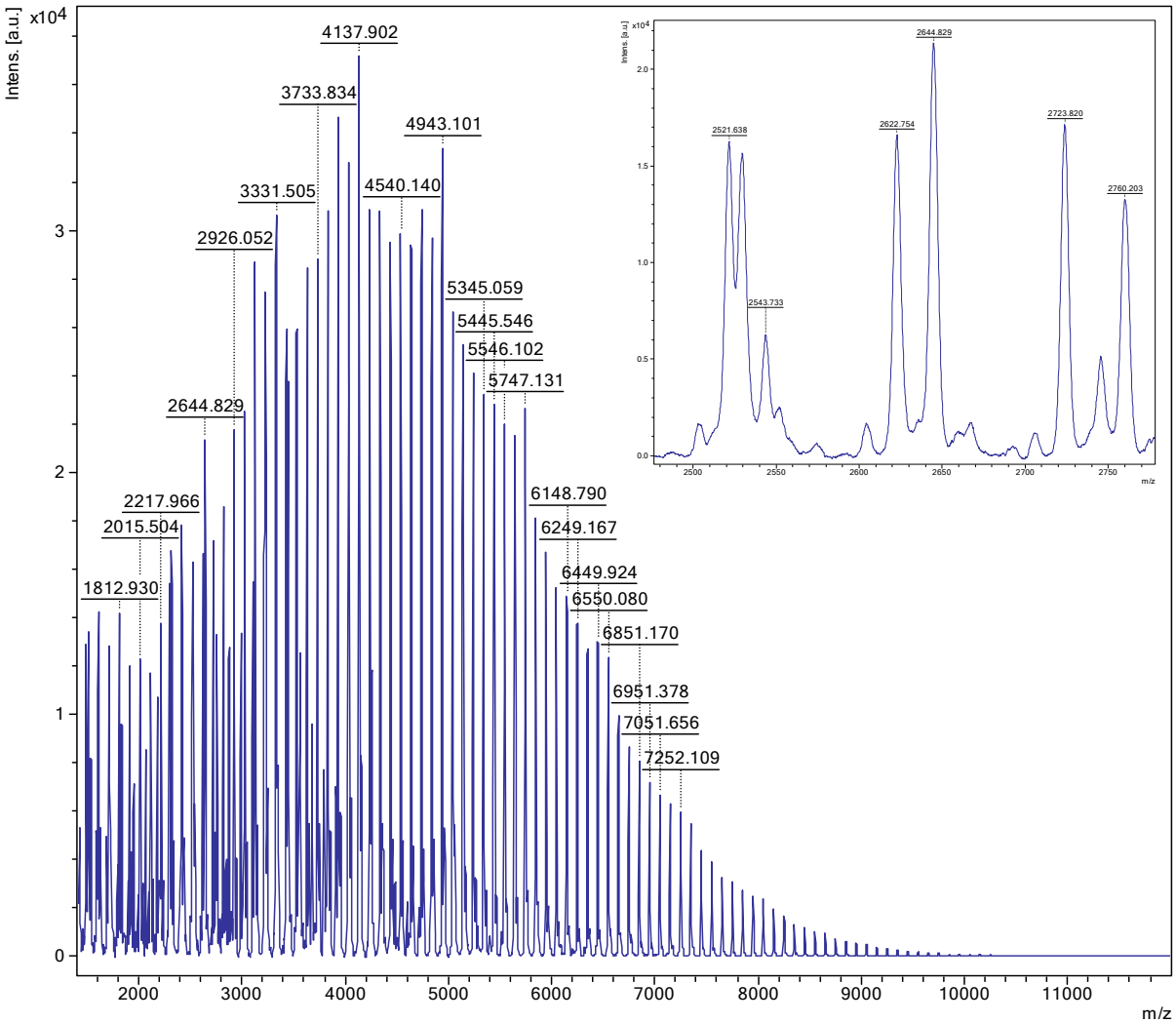

Figure S28. MALDI-ToF spectrum of PVL using LH_8 (entry 9, Table 1). Present are a family of linear polymers with HO/H end groups as sodium adducts, e.g. for n = 25, calc. = 2544, obsv. = 2543.7 and cyclic polymers as sodium adducts, e.g. for n = 27, calc. = 2726.2, obsv. = 2723.8.

Representative GPC traces

Zr8_melt_CL_500 to 1 to 4

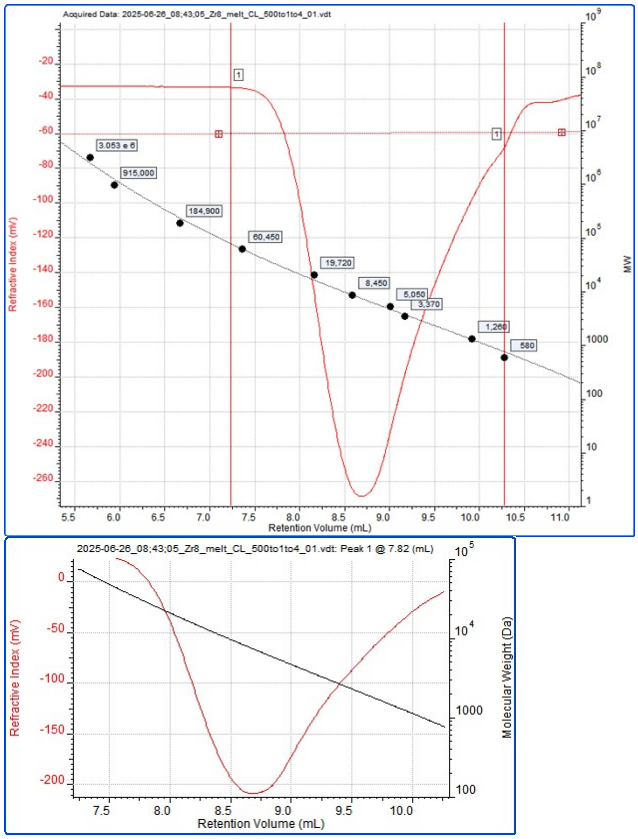

Figure S29. GPC trace for PCL using **1** as a melt (entry 3, Table 1).

Peak	1
Ret Vol (mL)	7.821
*M*n (Da)	4,082
*M*w (Da)	4,991
*M*z (Da)	-10791
*M*p (Da)	27,291
*M*w/*M*n	1.223

Zr8_VL_melt_500to1to4

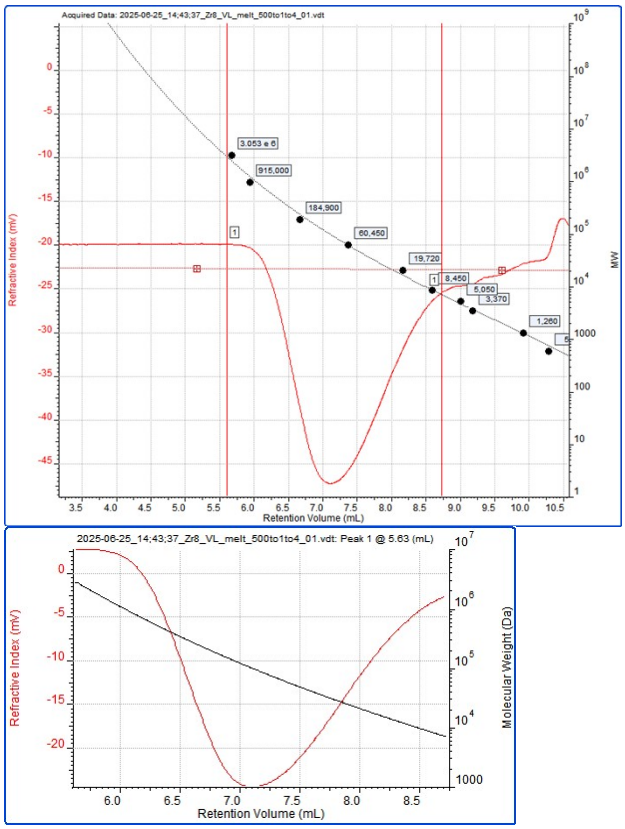

Figure S30. GPC trace for PVL using **1** as a melt (entry 8, Table 1)

Peak	1
Ret Vol (mL)	5.629
*M*n (Da)	41,102
*M*w (Da)	49,787
*M*z (Da)	-1651863
*M*p (Da)	2.672 e 6
*M*w/*M*n	1.211

calix8_CL_melt

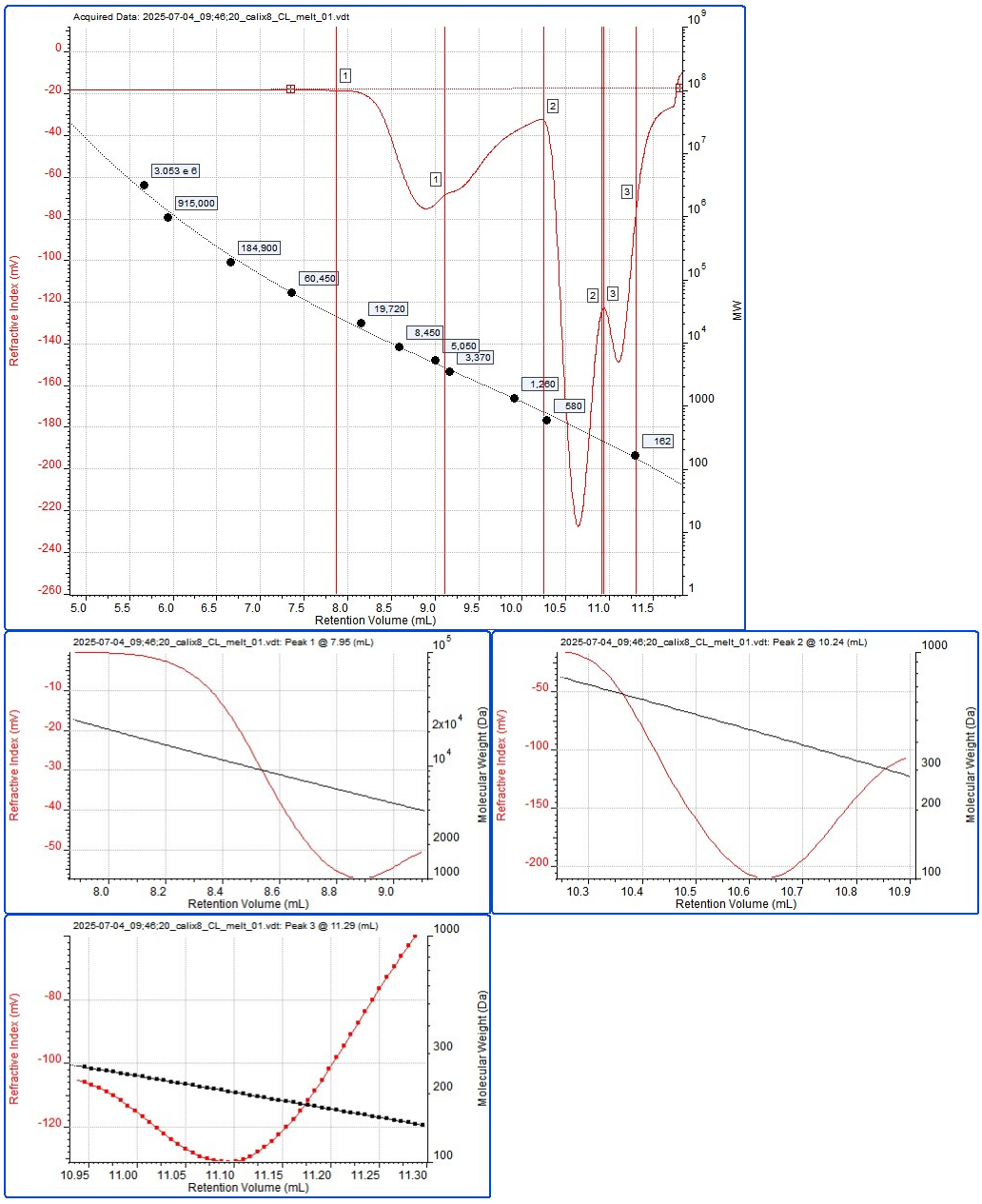

Figure S31. GPC trace for PCL using **LH_8** as a melt (entry 4, Table 1).

Peak	1	2	3
Ret Vol (mL)	7.950	10.241	11.288
*M*n (Da)	6,066	456	205
*M*w (Da)	6,677	490	210
*M*z (Da)	7,498	524	215
*M*p (Da)	22,051	772	147
*M*w/*M*n	1.101	1.073	1.027

8_VL_melt

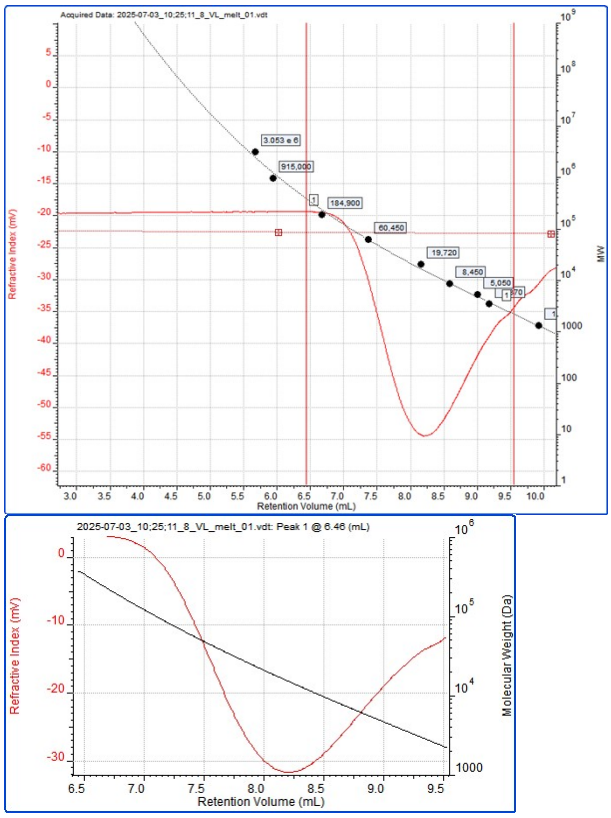

Figure S32. GPC trace for PVL using **LH_8** as a melt (entry 9, Table 1).

Peak	1
Ret Vol (mL)	6.455
*M*n (Da)	8,139
*M*w (Da)	9,519
*M*z (Da)	-150123
*M*p (Da)	363,578
*M*w/*M*n	1.169

$Zr(NMe_2)_4$_tol_110_500to1to4_VL

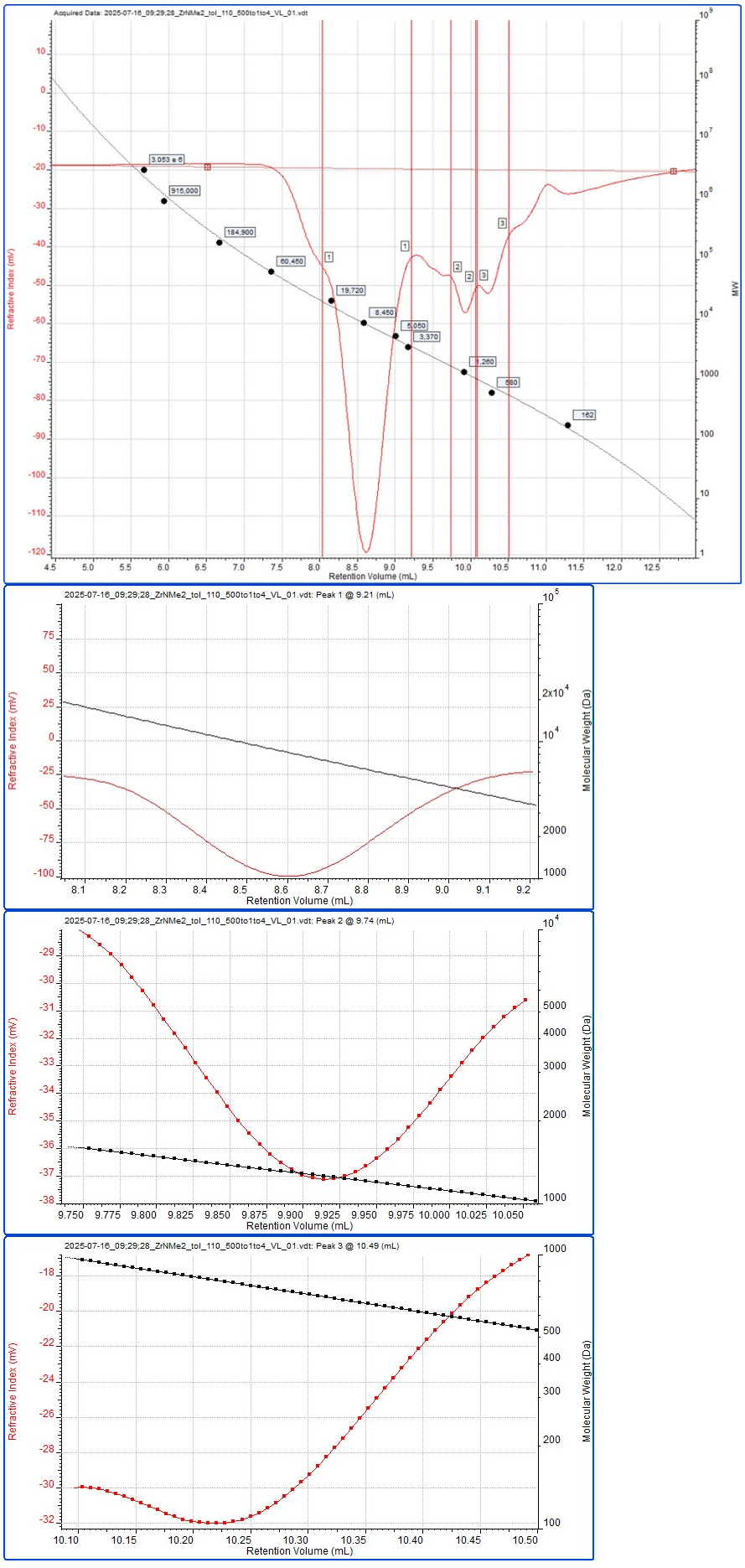

Figure S33. GPC trace for PVL using **[Zr(NMe$_2$)$_4$]** in toluene at 110 °C (entry 10, Table 1).

Peak	1	2	3
Ret Vol (mL)	9.209	9.740	10.491
*M*n (Da)	8,958	1,280	748
*M*w (Da)	10,806	1,301	769
*M*z (Da)	12,520	1,322	789
*M*p (Da)	3,426	1,597	536
*M*w/*M*n	1.206	1.016	1.028

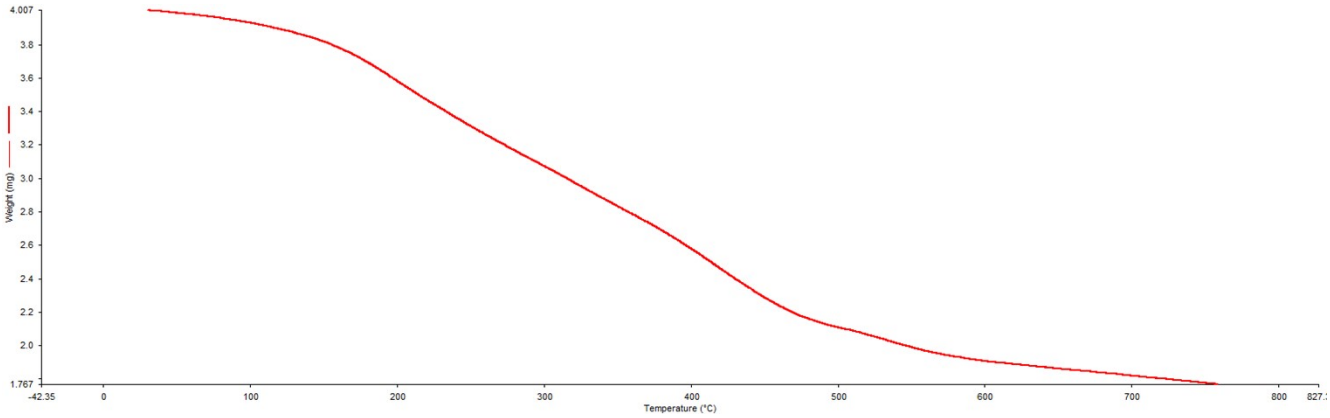

Figure S34. TGA of **1**.

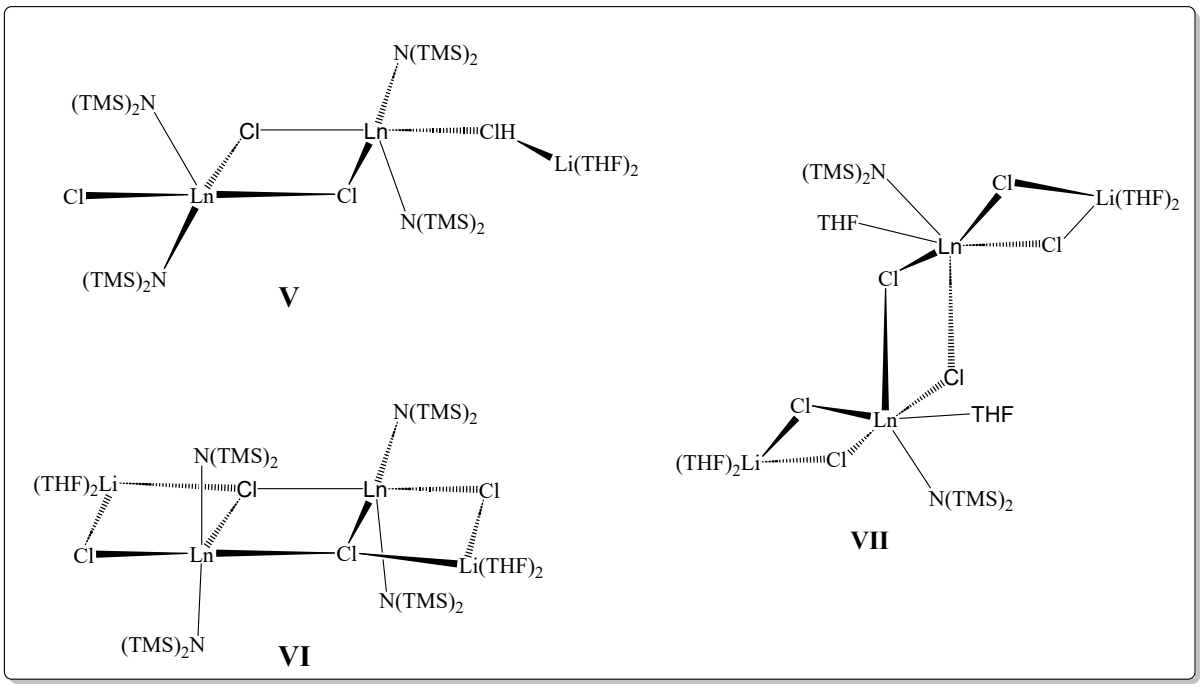

Figure S35. Lanthanide amides **V** to **VII**.[S5]

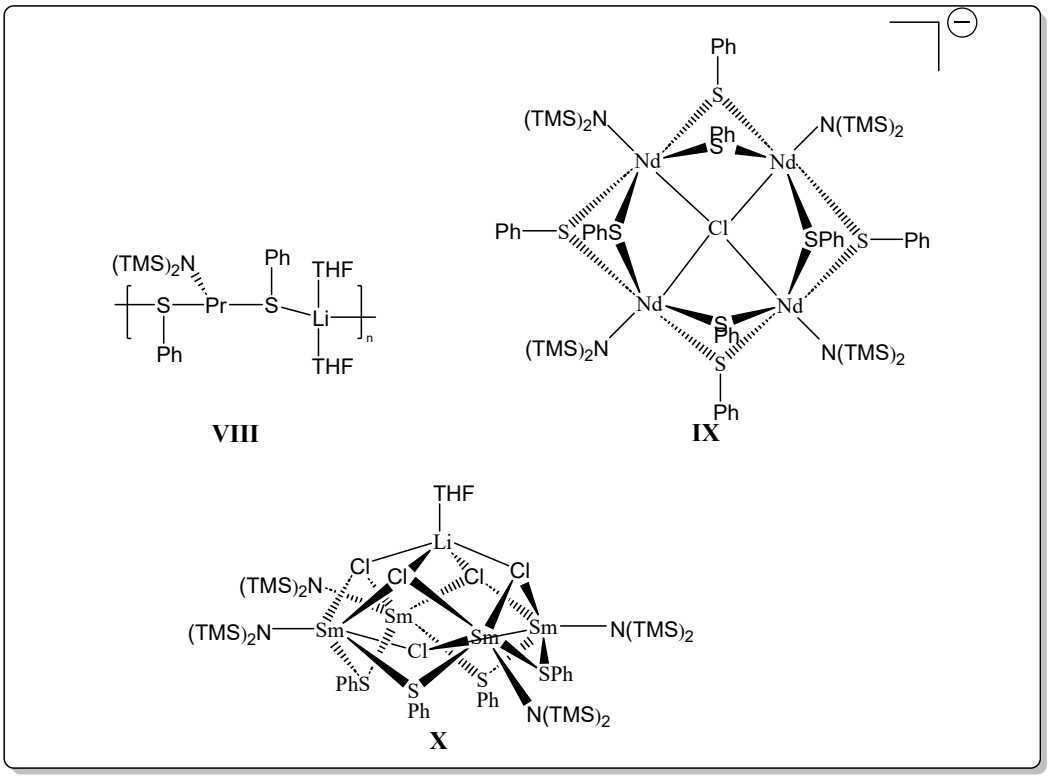

Figure S36. Lanthanide amide oligomers and polymers **VIII** – **X**. [S6]

References

[S1] V. Vaillant-Coindard, B. Théron, G. Printz, F. Chotard, C. Balan, Y. Rousselin, P. Richard, I. Tolbatov, P. Fleurat-Lessard, E. Bodio, R. Malacea-Kabbara, J. Bayardon, S. Dagorne and P. Le Gendre, Phenoxy-amidine ligands: toward lactic acid acid-tolerant catalysts for lactide ring opening polymerization. *Organometallics* 2022, **41**, 2920-2932. Doi: org/10.1021/acs.organomet.2c00343

[S2] B. Théron, V. Vaillant-Coindard, C. Balan, Y. Rousselin, J. Bayardon, R. Malacea-Kabbara and P. Le Gendre, Al and Zn phenoxy-amidine complexes for lactide ROP catalysis. *Dalton Trans*. 2023, **52**, 7854-7868. Doi: org/10.1039/D3DT01216F

[S3] Q. Gayden, R. Malacea-Kabbara, J. Bayardon, L. Plasseraud, M. Picquet, P. Le Gendre, B. Lagras and J. Kieffer, Synthesis of *N*,*N*-dimethylaminoethyl acrylate via a zinc phenoxyimine and phenoxyamidine complexes catalyzed transesterification reaction. *Appl. Organomet. Chem*. 2025, **39**, e70387. Doi: org/10.1002./aoc.70387

[S4] V. Vaillant-Coindard, J. Bayardon, Y. Rousselin, R. Malacea-Kabbara, J. -T. Pouzens, P. Fleurat-Lessard and P. le Gendre Prolinol-derived phenoxy-amidine titanium complexes in asymmetric silylcyanation of aldehydes. *Eur. J. Inorg. Chem*. 2025, **27**, e202400405. Doi: org/10.1002/ejic.202400405

[S5] H.-X. Li, Q.-F. Xu, J.-X. Chen, M.-L. Cheng, Y. Zhang, W.-H. Zhang, J.-P. Lang and Q. Shen, Syntheses, crystal structures and catalytic properties of a series of lanthanide(III) bis(trimethylsilyl)amide chloride complexes: $[\{((Me_3Si)_2N)_2Nd(\mu^{/}\text{-}Cl)Li(THF)_3\}(\mu\text{-}Cl)]_2$, $[\{((Me_3Si)_2N)_2Ln(\mu^{/}\text{-}Cl)Li(THF)_2\}(\mu\text{-}Cl)]_2$ (Ln = Eu, Ho), and $[\{(Me_3Si)_2NLn(\mu^{/}\text{-}$

$Cl)_2Li(THF)_2\}(\mu\text{-}Cl)]_2$ (Ln = Nd, Sm, Eu, Ho, Yb). *J. Organomet. Chem*. 2004, **689**, 3438-3448. Doi: 10.1016/j.jorganchem.2004.07.044

[S6] H.-X. Li, Z.-G. Ren, Y. Zhang, W.-H. Zhang, J.-P. Lang and Q. Shen, Construction of polymeric and oligomeric lanthanide(III) thiolates from preformed complexes $[(TMS)_2N]_3Ln(\mu\text{-}Cl)Li(THF)_3$ (Ln = Pr, Nd, Sm; $(TMS)_2N$ = bis(trimethylsilyl)amide). *J. Am. Chem. Soc*. 2005, **127**, 1122-1123. Doi: 10.1021/ja043415j